Int. J. of Geosynth. and Ground Eng. (2017) 3:12
DOI 10.1007/s40891-017-0089-3

ORIGINAL PAPER

The Effect of Olivine Content and Curing Time on the Strength of Treated Soil in Presence of Potassium Hydroxide

Mohammad Hamed Fasihnikoutalab[1] · Shahram Pourakbar[2] · Richard J. Ball[3] · Bujang Kim Huat[4]

Received: 8 February 2017 / Accepted: 20 April 2017 / Published online: 24 April 2017

Abstract When olivine (Mg_2SiO_4) is activated with potassium hydroxide (KOH), it acquires the ability to improve the unconfined compressive strength of soil. This paper investigates the use of olivine for soil stabilisation through alkaline activation by focusing on the role of different alkali activated olivine contents (5–20 wt%) in stabilising native soil at different curing durations. The strength results were supported by a detailed microstructural and compositional analysis including scanning electron microscopy, energy-dispersive X-ray spectroscopy and X-ray diffraction. Use of olivine in the presence of KOH increased the shear strength of soil up to 7.4 MPa in 90 days as a result of the formation of brucite, quartz and mullite in the structure of treated soil. This achievement implies a tremendous effect of olivine on the strength behaviour of treated soil. These results provide essential information which is significant from an environmental perspective as it offers a low energy alternative to existing technologies, for soil stabilisation.

Keywords Olivine · Alkaline activation · Soil stabilization · Microstructure analysis

✉ Mohammad Hamed Fasihnikoutalab
hfasih@gmail.com

[1] Department of Civil Engineering, University Putra Malaysia, 43400 Serdang, Selangor, Malaysia

[2] Department of Civil Engineering, University of Binaloud, No. 4 Moallem Street, Torghabeh, Mashhad, Iran

[3] Department of Architecture and Civil Engineering, BRE Centre for Innovative Construction Materials, University of Bath, Bath BA2 7AY, UK

[4] Department of Civil Engineering, University Putra Malaysia, 43400 Serdang, Selangor, Malaysia

Introduction

Application of cement as binder in soil stabilization is a widely used method for ground improvement [1–4]. However the high quantity of CO_2 released into the atmosphere is the main drawback of using cement [5]. The cement industry produces 5% of global man-made CO_2 emissions [6, 7]. Beside the emission of CO_2, another by-product of cement production is NO_x. Most of these nitrogen oxides are produced in cement kilns, which can contribute to the greenhouse effect and acid rain [8]. Several attempts involving the use of alternative methods or by-products as partial or full replacements of cement as stabilizers have been made to alleviate this. In this respect, binders based on alkali-activated materials have received a significant interest due to their sustainability advantages [9–15].

The alkali activation is a process in which, the aluminosilicate materials (industrial wastes and by-products) were dissolved through an alkaline activator such as sodium hydroxide (NaOH) or potassium hydroxide (KOH) [16]. Alkali-activated materials may have low (e.g. fly ash class F and metakaolin) or high (e.g. ground granulated blast-furnace slag (GGBS) and fly ash class C) calcium contents [17–20]. The formed geopolymeric gel can be viewed as an alkaline aluminosilicate base on amorphous Na^+ or K^+ aluminosilicate structure [21].

The literature already has an abundance of papers on alkaline-activation technology. In this regard, a number of studies were conducted to investigate the environmental benefits of alkaline-activated binder [22–24]; notably that of Weil et al. [25], who assessed the CO_2 emissions (kg CO_{2-eq}/m^3) and financial cost of alkali-activated binders. Those researchers reported that for an alkali-activated binder comprising 15.9% source binder dosage in the presence of high-alkali solutes, a reduction of 131 kg

CO_{2-eq}/m^3 was achieved for the combined feedstock and transport of the binders compared with that observed for cement. The results obtained so far show the effectiveness of alkali-activated binders for soil stabilization. In this regard, the effectiveness of alkali-activated fly ash (FA) as a source of silica and alumina for soil stabilization has been studied [26–30]. The feasibility of using metakaolin as an alkali-activated soil stabilizer at shallow depths was also studied [31]. These studies were conducted by mixing the above-mentioned binders with soft soils in the presence of NaOH and a silica-rich source such as sodium silicate as the alkaline activator. A recent studies by Pourakbar et al. [32] investigated the feasibility of using palm oil fuel ash (POFA) in the presence of high alkaline solutes (NaOH and KOH) for the purpose of soil stabilization. According to this investigation, a significant unconfined compressive strength (UCS) increase occurred at long curing times (90 days and 180 days of curing) when 10 M KOH was used as the best concentration for strength improvement of the soil. This was caused by the fact that K^+ has a larger size than the other alkaline metal cation, and therefore allows more dense and intimate polycondensation reactions, which substantially increase the overall long-term strength of the treated soil. In another attempt, Pourakbar et al. [33], have concluded that the inclusion of fiber reinforcement in alkali-activated POFA, regardless of their particular activator-precursor combinations, improved the postpeak behavior, by modifying the original brittle response into a more ductile behaviour.

Despite such positive findings, the above mentioned precursors (FA, POFA and metakaolin) are subjected to pre-treatment such as calcination and grinding to increase the reactivity of Al and Si present in binders [34–36]. The high temperatures utilized during the calcination process result in high energy usage and CO_2 emissions.

This paper focuses on the use of olivine (Mg_2SiO_4) to provide a more sustainable approach for the preparation of alkali activated binders to be used in soil stabilization. Olivine is a magnesium silicate, whose deposits are globally located [37]. It contains 45–49% magnesium oxide (MgO) and 40% SiO_2. Its weak nesosilicate structure and the absence of strong Si–O–Si bonds leaves olivine susceptible to dissolution and subsequent chemical reaction [38, 39]. Its high SiO_2 and alkaline metal content makes this natural resource an ideal candidate for alkali activation.

Due to its role as an effective source of MgO and SiO_2 with weak chemical bonds, olivine can be a good candidate for soil stabilization after being subjected to alkali activation. The aim of this study is to explore the use of olivine in the presence of KOH for the development of high strengths during soil stabilization. The behaviour of olivine treated soil was examined through UCS measurements. The composition and microstructure development of activated olivine treated soils were examined using scanning electron microscopy (SEM), energy-dispersive X-ray spectroscopy (EDX), X-ray diffraction (XRD).

Materials and Methods

Materials

Soil

According to the Unified Soil Classification System [40], the original soil is classified as high-plasticity clay (CH). Table 1 shows the physical and engineering properties of soil as-received and soil treated with different percentages of olivine. Table 2 lists the chemical composition of soil determined by X-ray fluorescence (XRF) analysis. Some of the main constituents are 28.5% SiO_2, 15.8% CaO, 8.3% Al_2O_3 and 0.25% MgO. The particle size distribution of the soil sample is shown in Fig. 1. The strength of this type of soil is often insufficient to enable its use in earth works or foundation layers, and thus constitutes an ideal challenge.

Table 1 Physical and engineering properties of soil

Properties	Value
Water content	
Optimum water content of soil	23.3%
Consistency limits	
Plastic limit	30%
Liquid limit	54%
Plasticity index	24%
Density	
Specific gravity of soil	2.65
Maximum dry density of soil	1.58 g/cm^3

Table 2 Chemical composition of silty clay soil determined by XRF

Fe_2O_3 (%)	SiO_2 (%)	CaO (%)	Al_2O_3 (%)	K_2O (%)	SO_3 (%)	MgO (%)	LOI (%)
33.7	28.5	15.8	8.3	4.45	3.75	0.25	5.25

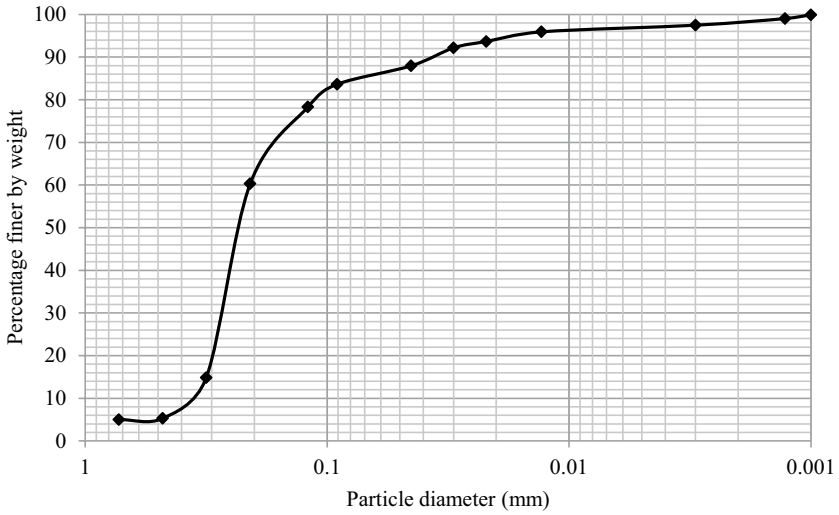

Fig. 1 Particle size distribution of soil

Table 3 Chemical composition of olivine determined by XRF

MgO (%)	SiO_2 (%)	Fe_2O_3 (%)	Al_2O_3 (%)	CaO	LOI (%)
48.3	40.3	8.9	1.4	–	1.1

Olivine

The olivine was obtained from MAHA chemical company in Malaysia. The chemical composition of olivine obtained using XRF is listed in Table 3. This olivine sample contains 48.3% MgO and 40.3% SiO_2. The D_{50} and SSA of olivine was 2.24 µm and 6.07 m^2/g, respectively.

Potassium Hydroxide

Potassium hydroxide (KOH), containing alkaline cation, was selected as activator because of its well-known efficiency. Although the price of NaOH is less than KOH, the authors used KOH as an alkali activator because K^+ has a larger size than the other alkaline metal cation, and therefore allows more dense and intimate polycondensation reactions, which substantially increase the overall long-term strength of the treated soil. These explanation is consistent with a study by Phair and Deventer [41]. According to those researchers' findings, matrices containing K^+ exhibited higher compressive strength and specific surface area and a lower degree of crystallinity in long curing regimes. This reagent was supplied in pellet form by the company R&M chemical and were previously diluted in distilled water to achieve a predesigned concentration. Note that the reaction with water of KOH is strongly exothermic, as with all strong bases. Thus, the alkaline solute was left to cool to ambient temperature before use.

Table 4 Mix compositions prepared under this study

Label	Olivine content (%)	Optimum water content (%)	Maximum dry density (gr/cm^3)	KOH/ Olivine ratio
KS	0	19.2	1.483	0
KO_5S	5	16	1.6	1.7
$KO_{10}S$	10	15	1.68	0.85
$KO_{15}S$	15	14.5	1.74	0.54
$KO_{20}S$	20	14	1.79	0.39

Methods

Mix Composition and Sample Preparation

The compositions of the various mixes of soil, olivine, KOH and water prepared under this study are given in Table 4. Mix labelled "KS" represents an alkali treated soil. Mixes labelled KO_BS represent as alkali treated soils containing B: 5, 10, 15 and 20% of olivine respectively at different curing time of 7 and 90 days. The concentration of KOH was fixed at 10 M for all samples according to the findings of previous studies [27, 29, 42].

The alkali activator was dissolved in distilled water at a predetermined concentration. The solution prepared was left to cool down for 24 h before being added to the olivine and soil mixture. The soil was air-dried before mixing to remove any remaining moisture. All specimens were cured in plastic bags for 7 and 90 days to prevent any changes in the initial water content due to evaporation. Note that the optimum water content (OWC) corresponding to maximum dry density (MDD) was determined for each mix composition (Table 4).

Unconfined Compressive Strength

To prepare the samples, alkali activators were dissolved in distilled water at predetermined concentrations to avoid the effect of unknown contaminants in the mixing water. The dry soil was initially mixed with the olivine and activator solution was then added to the solids accoriding to OWC and MDD of each percanatge of olivin in soil and thoroughly mixed until a uniform blend was achieved. After de-moulding, all specimens were cured in plastic bags for 7 and 90 days to prevent changes in water content due to evaporation. Finally, the UCS measurements were conducted on the prepared samples with a diameter of 50 mm and a height of 100 mm according to BS 1924: Part 7 [43] in three different specimens, and the results were accepted only if deviated <5% from the average. The equipment used for this purpose was an Instron 3300, operated at a loading rate of 100 kN/min.

Microstructural Analysis

Samples were examined in a presence of KOH by using a JSM 5700 SEM coupled with an EDX spectrometer. Samples were sputter coated with gold using a Emitech K550X Sputter Coater before analysis to increase the electrical conductivity of the surface and reduce charging. Crystalline phases were investigated using a Philips X-Ray diffractometer equipped with X'Pert software over a 2-theta range of 3°–50° Cu K alpha.

Results and Discussion

Strength Development

Figure 2 shows the stress–strain behaviour of soil (S), alkali-activated soil (KS) and alkali-activated soil (KO_BS) with different percentages of olivine (5, 10, 15, and 20) after 7 days of curing. Untreated soil specimens (S) showed a ductile behaviour with strength of 103.4 kPa at a failure strain of around 1.8%. Alkali activation improved the strength of the soil with strengths reported as 292 kPa after 7 days of curing. Furthermore, the stress–strain behaviour of alkali activated olivine treated soil increased by increasing the olivine percentages of 5, 10, 15 and 20%. According to Fig. 2 the strength of alkali activated olivine treated soil after 7 days of curing was 389, 550, 675 and 953 kPa for KO_5S, $KO_{10}S$, $KO_{15}S$ and $KO_{20}S$ samples, respectively.

Figure 3 shows the stress–strain behaviour of alkali-activated soil (KS) and alkali-activated olivine treated soil after a curing time of 90 days. This figure shows the strength of the soil increased to 5.05, 5.27, 6.71 and 7.4 MPa for the KO_5S, $KO_{10}S$, $KO_{15}S$ and $KO_{20}S$ samples respectively. A

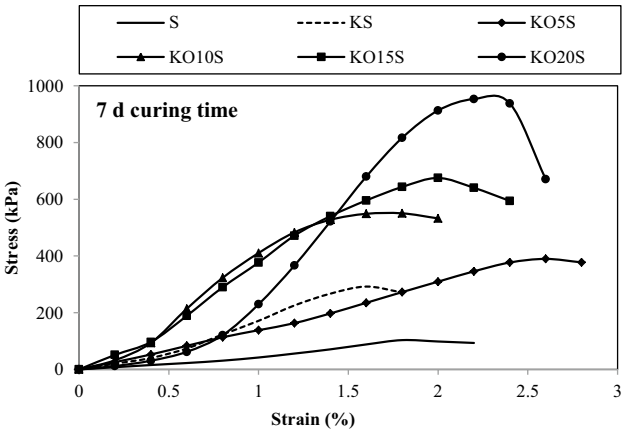

Fig. 2 UCS of 0, 5, 10, 15 and 20 of olivine treated soil in the presence of 10 M KOH after 7 day curing times

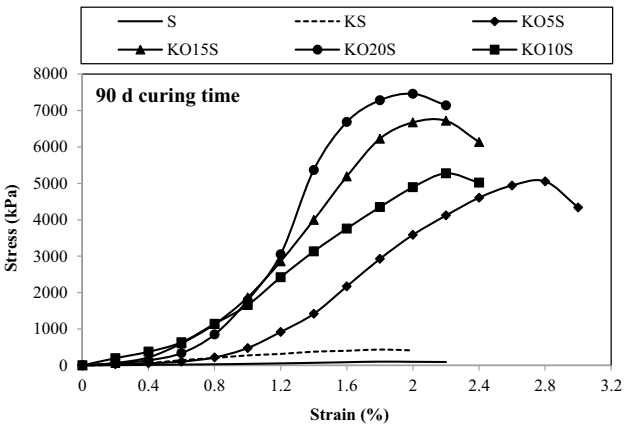

Fig. 3 UCS of 0, 5, 10, 15 and 20 of olivine treated soil in the presence of 10 M KOH after 90 day curing times

rapid increase in the strength of soil specimens in the presence of KOH was observed over time, which was attributed to the role of KOH in promoting the dissolution of Si and Al present in soil [29]. The increase in the strength of KS after 7 and 90 days curing was not significant due to the low reactivity of Si and Al. A progressive increase in strength was observed when different amounts of olivine were added to the mixture. The strength of samples increased with olivine content (0–20%) and curing time (7 and 90 days). In this respect, $KO_{20}S$ achieved the highest strength within all alkali treated soil samples after 7 and 90 days of curing. The important role of olivine in the strength development of soil samples was obvious as significant increases in strength were observed with an increase in the olivine content. Figure 3 shows that alkali-activated specimens achieved higher strengths after 90 days of curing. The rate of increase was almost constant at all ages although it augmented as the olivine content increased to 20%.

The underlying mechanisms responsible for the strength development of the soils after alkali treatment can be explained in terms of the reactions that take place during alkali activation. When olivine is mixed with KOH within a soil mix, the KOH solution leaches the silicon from amorphous phases. The formation of $Mg(OH)_2$ is an expansive process, which fills the available pores in the soil, thereby increasing the density and final strength. The presence of KOH can result in the leaching of the Si and Al in the amorphous phases of soil, producing an alumina-silica-hydrate (A-S-H) gel.

Previous studies have shown that the addition of calcium (Ca) generally has a positive effect on the mechanical properties of alkali activated binders [33, 44]. Calcium ions are capable of acting as a charge-balancing cation within the alkali-activated binder structure. It was also proposed that the simultaneous formation of A-S-H and C-S-H gels may contribute to an increase in the compressive strength of the matrix [45]. Therefore, besides Si and Al, Mg ions may play a significant role in crystal growth. In the presence of an alkali activator, Mg ions could provide additional nucleation sites for the precipitation of dissolved species and contribute to the formation of magnesium silicate hydrate (M-S-H) gel [21, 46, 47]. The strength development of the prepared samples could be attributed to these reactions.

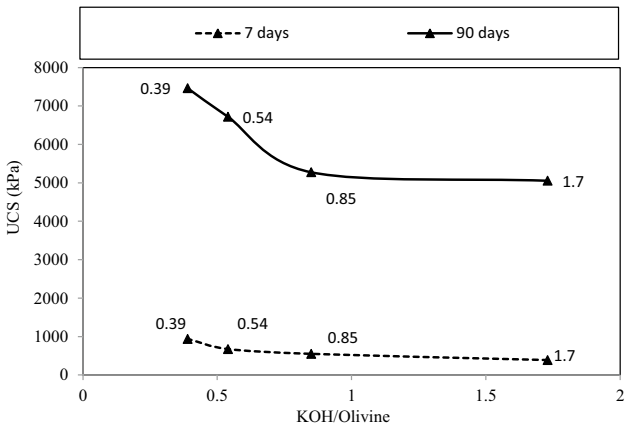

Fig. 4 Influence of KOH/Olivine weight ratio on strength development at 7and 90 day

Figure 4 shows the variation in UCS after 7 and 90 days curing time with the KOH and olivine (KOH/olivine) mass ratio ranging between 0.39 and 1.7. Strength generally increased as the KOH/olivine weight ratio decreased. The maximum UCS level was obtained at the lowest KOH/olivine ratio of 0.39 for all curing periods. These findings are consistent with the existing literature, which report an increase in strength with a reduction in activator/source binder ratios [27, 29, 36, 48]. This might be explained by using the dry unit weight-liquid content relationship theory for soil stabilization. According to Table 4, the highest MDD and the lowest OWC were obtained when the KOH/Olivine ratio was at a minimum.

SEM Characterization of Olivine Treated Soil in the Presence of KOH

As can be seen in Fig. 5a, b, the SEM analysis was performed on untreated soil and selected treated specimens that obtained the highest strength ($KO_{20}S$) after a curing time of 90 days, based on pervious study by Fasihniukotalab et al. [15], the 20% of olivine has a highest strength among other dosages. As can be clearly seen in this Fig. 5b, the microstructure of treated soil consists of soil particles

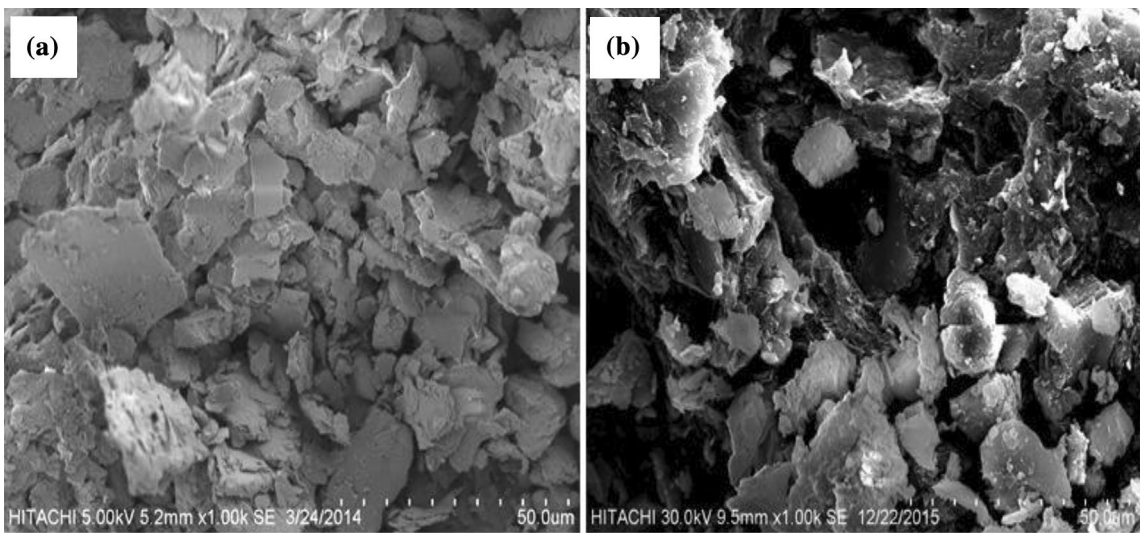

Fig. 5 SEM images of **a** untreated soil (S) and **b** $KO_{20}S$ -sample after 90 day curing

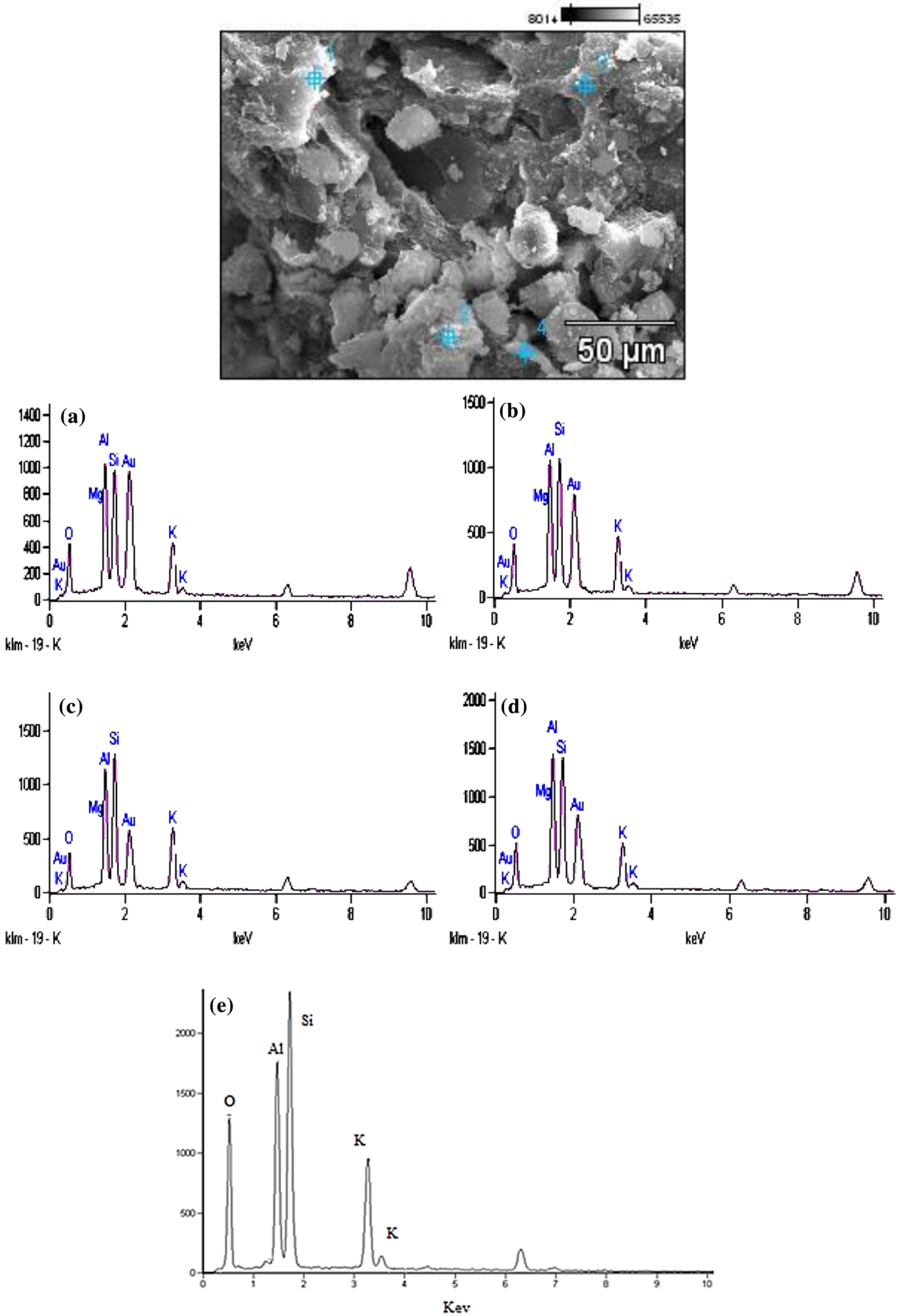

Fig. 6 EDX analysis of samples: **a** KO_5S, **b** $KO_{10}S$, **c** $KO_{15}S$, **d** $KO_{20}S$ and **e** KS after 90 days curing

and the irregular shape of olivine particles in the presence of 10 M KOH after 90 day curing time. SEM images demonstrate a compact morphology without any major discontinuities, which is consistent with the mechanical properties observed (Fig. 3). This is because the addition of KOH to the olivine treated soil and reaction between MgO and SiO_2 in the olivine which led to the production of $Mg(OH)_2$. These results match those observed in earlier studies showing that using $Mg(OH)_2$ in soil stabilization produces a dense surface structure for soil and the formation of $Mg(OH)_2$ fills in the available pore space [5, 49, 50]. Accordingly the previous studies have shown that the

Table 5 The EDX and UCS results of olivine treated soil in the presence of 10 M of KOH after 90 days curing

Sample	Si/Al molar ratio	K/Al molar ratio	Mg/Al molar ratio	SiO_2/K_2O ratio	UCS (MPa)
KO_5S	1.23	0.67	1.5	3.25	5.05
$KO_{10}S$	1.4	0.77	1.55	2.39	5.27
$KO_{15}S$	1.59	0.85	1.61	2	6.71
$KO_{20}S$	1.82	1.05	1.75	1.8	7.46

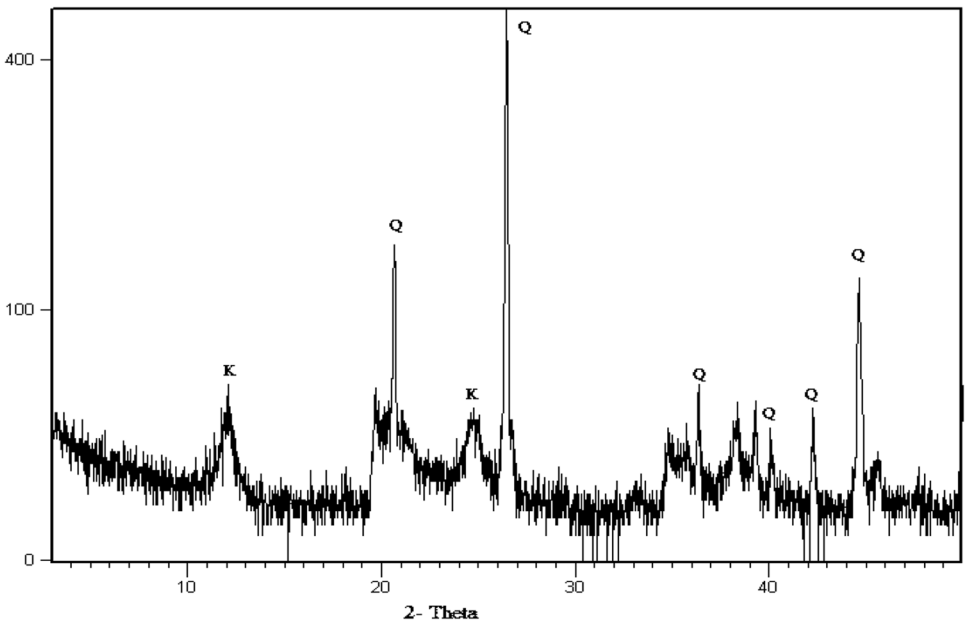

Fig. 7 The XRD of untreated soil (*K* kaolinite, *Q* quartz)

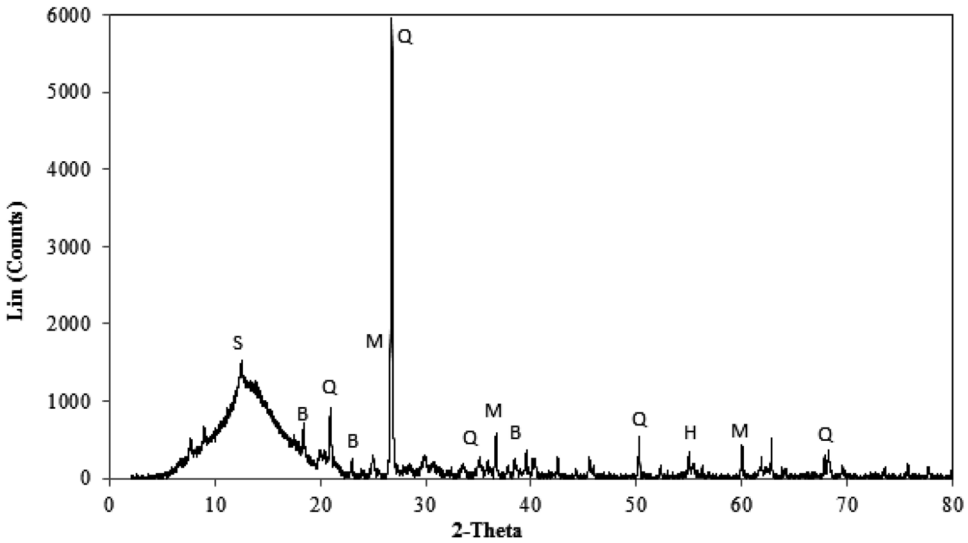

Fig. 8 The XRD of $KO_{20}S$ after 90 day curing time (*B* brucite, *H* hematite, *M* mullite, *S* serpentine, *Q* quartz)

produced gels were leached clay and Fly ash particles in soil and made strong bond among clay particles as a result of forming relatively dense alumino-silicate gels [51].

EDX Characterization of Olivine Treated Soil in the Presence of KOH

Figure 6a–d shows the EDX analysis of—KO_5S, $KO_{10}S$, $KO_{15}S$ and $KO_{20}S$ after 90 days of curing respectively. As shown in this figure, the most common phases observed contain the elements such as K, Si and Al, suggesting the formation of a silicate-activated gel as a result of the activation process. Table 5 lists the molar ratios of Si/Al, K/Al, Mg/Al and SiO_2/K_2O of the samples analysed under EDX. An increase in the strength of soils was observed with an increase in the Si/Al, K/Al ad Mg/Al ratios, which was in line with previous studies that showed higher strengths at Si/Al ratios ranging between 1.15 and 2.15 [28, 52–54]. This corresponded to a higher degree of geopolymerization because of the higher K/Al ratio. Moreover, K^+ cations also played a role in balancing the net negative charge of Al^{3+} resulting from the Al:O coordination [9, 27, 55, 56].

XRD Characterization of Olivine Treated Soil in the Presence of KOH

Figures 7 and 8 show the XRD of untreated soil and 20% olivine treated soil after 90 days of ambient curing. The roughly peaks of 11.5 and 24.5 for kaolinite and of 21, 26, 36, 40 and 44.5 for quartz are identified at untreated soil. Furthermore, the roughly peaks of (18, 23 and 39) shows the brucite, (21, 27, 51 and 68) shows the quartz, serpentine identified as peak of 13, (26, 37 and 60) shows the mullite, and hematite (55) are identified as a result of 20% olivine dissolution through reaction with the KOH present in the soil. One important conclusion that may be drawn from the observation of the diffractogram in Fig. 8 is that when KOH is added to the olivine treated soil, the formation of $Mg(OH)_2$, SiO_2, and mullite can be observed. As can be seen in Fig. 7, peaks at 2-theta values of 20, 26, 34, 50 and 67 indicate the presence of quartz (SiO_2), and those at 18, 21, 36 correspond to magnesium hydroxide $Mg(OH)_2$ Moreover, peaks of 12 and 54 indicate serpentine and hematite respectively in the XRD [27, 49, 57].

Conclusions

This study has investigated the role of alkali activated olivine treated soil. The results indicate that olivine can be used as a sustainable precursor in alkali activated treated soil. The following conclusions can be drawn:

- The strength of olivine treated soil in the presence of KOH increased with olivine content and curing time, reaching a value up to 7.4 MPa after 90 day curing. In this respect, the duration of curing has a direct effect on the amount of activated reactants transformed into the binding products. This high strength development implies the dissolution of olivine through the addition of KOH. XRD diffractograms and SEM images confirmed the formation of $Mg(OH)_2$ as a result of the hydration of magnesium in olivine treated soil.
- The dissolution mechanism of olivine and the influence of Si/Al, K/Al and SiO_2/K_2O ratios of alkali activated systems led to an increase in strength as confirmed by EDX results.
- This study has identified the successful use of olivine for soil stabilization in the presence of strong alkaline activators like KOH.

Acknowledgements The authors sincerely give thanks to the University Putra Malaysia and Fundamental Research Grant Scheme (FRGS/1/2015/TK01/ UPM/01/2) entitled 'Sustainable soil stabilisation by olivine and its mechanisms' funded by the Ministry of Higher Education in Malaysia (Project ID 93474–135837) for financial support of this research. Moreover, authors would like to extend their sincerest thanks and appreciation to Dr. Gabriele Kociok-Köhn from University of Bath, Department of Chemistry who helped us accomplish of XRD analysis and Dr. Afshin Asadi from University Putra Malaysia for this study.

References

1. Farouk A, Shahien MM (2013) Ground improvement using soil–cement columns: experimental investigation. Alexandria Eng J 52(4):733–740
2. Horpibulsuk S (2012) Strength and microstructure of cement stabilized clay. INTECH
3. Yi Y, Liska M, Unluer C, Al-Tabbaa A (2013) Initial investigation into the carbonation of MgO for soil stabilisation. Proc 18th Int Conf Soil Mech Geotech Eng 5:2641–2644
4. Pourakbar S, Asadi A, Huat BBK, Fasihnikoutalab MH (2015) Stabilization of clayey soil using ultrafine palm oil fuel ash (POFA) and cement. Transp Geotech 3:24–35
5. Yi Y, Liska M, Akinyugha A, Unluer C, Al-Tabbaa A (2013) Preliminary laboratory-scale model auger installation and testing of carbonated soil-MgO column. Geotech Test J 36(3):1–10
6. Friedlingstein P, Andrew RM, Rogelj J, Peters GP, Canadell JG, Knutti R, Luderer G, Raupach MR, Schaeffer M, van Vuuren DP, Le Quere C (2014) Persistent growth of CO2 emissions and implications for reaching climate targets. Nat Geosci 7(10):709–715
7. Ke J, Mcneil M, Price L, Khanna NZ (2013) Estimation of CO_2 emissions from China' s cement production: methodologies and uncertainties methodologies and uncertainties. Energy Policy 57:172–181
8. Hendriks P, Worrell CA, De Jager D, Blok K, Riemer (1998) Emission reduction of greenhouse gases from the cement industry. In Proceedings of the 4th International Conference on Greenhouse Gas Control Technologies, Interlaken

9. Duxson P, Fernández-Jiménez A, Provis JL, Lukey GC, Palomo A, Deventer JSJ (2007) Geopolymer technology: the current state of the art. J Mater Sci 42(9):2917–2933
10. Gartner E (2004) Industrially interesting approaches to 'low-CO_2' cements". Cem Concr Res 34(9):1489–1498
11. Turner LK, Collins FG (2013) Carbon dioxide equivalent (CO_2-e) emissions: a comparison between geopolymer and OPC cement concrete. Constr Build Mater 43:125–130
12. Pourakbar S, Huat BBK, Fasihnikoutalab MH, Asadi A (2015) Soil stabilisation with alkali-activated agro-waste. Environ Geotech 2(6):359–370
13. Fasihnikoutalab MH, Westgate P, Huat BBK, Asadi A, Ball RJ, Haslinda N, Singh P (2015) New insights into potential capacity of olivine in ground improvement. Electron J Geotech Eng 20(8):2137–2148
14. Fasihnikoutalab MH, Asadi A, Bujang KH, Westgate P, Ball RJ, Pourakbar S (2015) Laboratory-scale model of carbon dioxide deposition for soil stabilization. J Rock Mech Geotech Eng 8(2):178–186
15. Fasihnikoutalab MH, Asadi A, Bujang KH, Ball RJ, Pourakbar S, Parminder S (2015) Utilization of carbonating olivine for soil stabilization. Environ Geotech. doi:10.1680/jenge.15.00018
16. Duxson P, Provis JL (2008) Designing precursors for geopolymer cements. J Am Ceram Soc 91(12):3864–3869
17. Rajamma R, Labrincha JA, Ferreira VM (2012) Alkali activation of biomass fly ash–metakaolin blends. Fuel 98:265–271
18. Rashad AM (2013) Alkali-activated metakaolin: a short guide for civil Engineer—An overview. Constr Build Mater 41:751–765
19. Buchwald A, Hilbig H, Kaps C (2007) Alkali-activated metakaolin-slag blends—performance and structure in dependence of their composition. J Mater Sci 42(9):3024–3032
20. Bernal SA, Mejía de Gutiérrez R, Provis JL (2012) Engineering and durability properties of concretes based on alkali-activated granulated blast furnace slag/metakaolin blends. Constr Build Mater 33:99–108
21. Yip CK, Lukey GC, Provis JL, van Deventer JSJ (2008) Effect of calcium silicate sources on geopolymerisation. Cem Concr Res 38:554–564
22. Van Jaarsveld JGS, Van Deventer JSJ, Lorenzen L (1997) The potential use of geopolymeric materials to immobilise toxic metals: Part I. Theory and applications. Miner Eng 10(7):659–669
23. Habert G, d'Espinose de Lacaillerie JB, Roussel N (2011) An environmental evaluation of geopolymer based concrete production: reviewing current research trends. J Clean Prod 19(11):1229–1238
24. Ng TS, Voo YL, Foster SJ, (2012) Sustainability with ultra-high performance and geopolymer concrete construction. In: Fardis M (ed) Innovative materials and techniques in concrete construction, Springer Science+Business Media, Dordrecht, pp 81–100
25. Weil M, Dombrowsk K, Buchawald A (2009) Life-cycle analysis of geopolymers. Geopolymers, structure, processing, properties and applications. Woodhead Publ Ltd 5(3):194–210
26. Cristelo N, Glendinning S, Fernandes L, Pinto AT (2012) Effect of calcium content on soil stabilisation with alkaline activation. Constr Build Mater 29:167–174
27. Cristelo N, Glendinning S, Miranda T, Oliveira D, Silva R (2012) Soil stabilisation using alkaline activation of fly ash for self compacting rammed earth construction. Constr Build Mater 36:727–735
28. Cristelo N, Glendinning S, Fernandes L, Pinto AT (2013) Effects of alkaline-activated fly ash and Portland cement on soft soil stabilisation. Acta Geotech 8(4):395–405
29. Cristelo N, Glendinning S, Pinto AT (2011) "Deep soft soil improvement by alkaline activation". Proc ICE-Gr Improv 164(1):1–10
30. Ryu GS, Lee YB, Koh KT, Chung YS (2013) The mechanical properties of fly ash-based geopolymer concrete with alkaline activators. Constr Build Mater 47:409–418
31. Zhang M, Guo H, El-Korchi T, Zhang G, Tao M (2013) Experimental feasibility study of geopolymer as the next-generation soil stabilizer. Constr Build Mater 47:1468–1478
32. Pourakbar S, Huat BBK, Asadi A, Fasihnikoutalab MH (2016) Model study of alkali-activated waste binder for soil stabilization. Int J Geosynth Gr Eng 2(4):35
33. Pourakbar S, Asadi A, Huat BBK, Cristelo N, Fasihnikoutalab MH (2016) Application of alkali-activated agro-waste reinforced with wollastonite fibers in soil stabilization. J Mater Civ Eng 29(2):1–11
34. Li C, Sun H, Li L (2010) A review: the comparison between alkali-activated slag (Si + Ca) and metakaolin (Si + Al) cements. Cem Concr Res 40(9):1341–1349
35. Weng L, Sagoe-Crentsil K (2007) Dissolution processes, hydrolysis and condensation reactions during geopolymer synthesis: part I—low Si/Al ratio systems. J Mater Sci 42(9):2997–3006
36. Duxson P, Mallicoat SW, Lukey GC, Kriven WM, van Deventer JSJ (2007) The effect of alkali and Si/Al ratio on the development of mechanical properties of metakaolin-based geopolymers. Colloids Surf A 292(1):8–20
37. TARGET MAP (2012) Olivine distribution resources. MapGenia [Online]. http://www.targetmap.com/viewer.aspx?reportId=24272.
38. Schuiling RD (2013) Olivine: a supergreen fuel. Energy Sustain Soc 3(18):1–4
39. Schuiling R (2001) Olivine, the miracle mineral. Mineral J 23(5/6):81–83
40. ASTM International (2006) Standard practice for classification of soils for engineering purposes (unified soil classification system), vol. D2487. ASTM Standard Guide, Philadelphia, pp 1–5
41. Phair J, Van Deventer J (2001) Effect of silicate activator pH on the leaching and material characteristics of waste-based inorganic polymers. Mineral Eng 14(3):289–304
42. D Bondar, CJ Lynsdale, NB Milestone, N Hassani, AA Ramezanianpour (2011) Effect of type, form, and dosage of activators on strength of alkali-activated natural pozzolans. Cem Concr Compos 33(2):251–260
43. British Standard Institution, British Standard Methods of test for Soils for civil engineering purposes. Part 7: Shear strength tests (total stress). BS 1377-7:1990, No. August, 1999
44. Temuujin J, van Riessen A, Williams R (2009) Influence of calcium compounds on the mechanical properties of fly ash geopolymer pastes. J Hazard Mater 167(1–3):82–88
45. Winnefeld F, Leemann A, Lucuk M, Svoboda P, Neuroth M (2010) Assessment of phase formation in alkali activated low and high calcium fly ashes in building materials. Constr Build Mater 24(6):1086–1093
46. Yip CK, Van Deventer JSJ (2003) Microanalysis of calcium silicate hydrate gel formed within a geopolymeric binder. J Mater Sci 38(18):3851–3860
47. Salih MA, Abang Ali AA, Farzadnia N (2014) Characterization of mechanical and microstructural properties of palm oil fuel ash geopolymer cement paste. Constr Build Mater 65:592–603
48. Fasihnikoutalab MH, Asadi A, Unluer C, Huat BK, Ball RJ, Pourakbar S (2017) Utilization of alkali-activated olivine in soil stabilization and the effect of carbonation on unconfined compressive strength and microstructure. J Mater Civ Eng. doi:10.1061/(ASCE)MT.1943-5533.0001833
49. Yi Y, Liska M, Unluer C, Al-Tabbaa A (2013) Carbonating magnesia for soil stabilization. Can Geotech J 50(8):899–905
50. Zhu J, Ye N, Liu J, Yang J (2013) Evaluation on hydration reactivity of reactive magnesium oxide prepared by calcining magnesite at lower temperatures. Ind Eng Chem Res 52(19):6430–6437

51. Rattanasak U, Chindaprasirt P (2009) Influence of NaOH solution on the synthesis of fly ash geopolymer. Mineral Eng 22(12):1073–1078
52. Duxson P, Provis JL, Lukey GC, van Deventer JSJ (2007) The role of inorganic polymer technology in the development of 'green concrete'. Cem Concr Res 37(12):1590–1597
53. Fernández-Jiménez A, Palomo A, Criado M (2005) Microstructure development of alkali-activated fly ash cement: a descriptive model. Cem Concr Res 35(6):1204–1209
54. Wang SD, Scrivener KL (2003) 29Si and 27Al NMR study of alkali-activated slag. Cem Concr Res 33:769–774
55. Fernández-Jiménez A, Palomo A (2005) Composition and microstructure of alkali activated fly ash binder: Effect of the activator. Cem Concr Res 35(10):1984–1992
56. Zhang M, El-Korchi T, Zhang G, Liang J, Tao M (2014) Synthesis factors affecting mechanical properties, microstructure, and chemical composition of red mud–fly ash based geopolymers. Fuel 134:315–325
57. Komljenović M, Bascarević Z, Bradić V (2010) Mechanical and microstructural properties of alkali-activated fly ash geopolymers. J Hazard Mater 181(1–3):35–42